Available online at www.sciencedirect.com
ScienceDirect
Solid State Communications 145 (2008) 447–450
solid state communications
www.elsevier.com/locate/ssc

Ballistic Aharonov–Bohm quantum bits and quantum gates

Leo Yu, Oleksandr Voskoboynikov*

National Chiao Tung University, 1001 Ta Hsueh Road, Hsinchu, 300, Taiwan

Received 2 October 2007; received in revised form 27 November 2007; accepted 17 December 2007 by S. Miyashita
Available online 7 January 2008

Abstract

We propose an architecture to perform quantum computation, using ballistic electrons as qubits and coupled quantum rings as quantum gates. In the proposed architecture two adjacent one-dimensional wires, creating a single qubit, are connected to two coupled quantum rings, where the required magnetic flux is provided by enclosed nano-sized magnets. The phase modulation of the wave function of the ballistic electrons under the Aharonov–Bohm effect is carefully designed to facilitate reprogrammable and dynamically controllable quantum gates. Arbitrary single-qubit quantum gates with high fidelity can be constructed on the basis of this architecture.

PACS: 73.23.-b; 73.23.Ad

Keywords: D. Mesoscopic systems; D. Aharonov–Bohm effect; D. Quantum bit

The physical implementation of a quantum computer continues to pose a great challenge. Among the numerous schemes to implement quantum computers, solid state micro- and nano-systems draw special attention because of their obvious advantages: scalability, miniaturizability and flexibility in design. Quantum computation using ballistic electrons has been proposed recently as an attractive candidate [1–3]. While relying on the interference of quantum waves to implement quantum gates, most previous proposals have not explored in depth the use of a magnetic field to modulate the phases of the ballistic electrons (the Aharonov–Bohm (AB) effect [4]). So, we propose in this paper a system of one-dimensional (1D) quantum wires incorporating an array of nano-rings and nano-sized magnets [5] which can act as a new architecture to perform quantum computation. Each quantum gate in this architecture is controlled dynamically by flipping the magnetization of the nano-sized magnets and changing the chemical potential for the ballistic electrons. This provides the opportunity to program dynamically a quantum computer the same way as we do a classical one.

In our architecture we use ballistic electrons as flying qubits in one-dimensional quantum wires within the dual rail representation [3,6]. The architecture is shown conceptually in Fig. 1. A pair of adjacent quantum rings, which enclose nano-sized magnets (represented in Fig. 1 as tablets with arrows), stands for a single-qubit AB quantum gate (basic element). Fig. 1 shows two single-qubit gates and a controlled phase shifter [3]. The controlled phase shifter enables the entangling of two single qubits and the formation of a two-qubit gate [3,7]. During a quantum computation cycle, two input qubits enter from the two pairs of parallel 1D quantum wires at the left-hand side (the rails) of two AB quantum gates. Their wave functions interfere and become modulated under the AB effect in the quantum rings, then they leave and enter finally the two pairs of parallel 1D quantum wires at the right-hand side. Note that the two pairs of quantum wires at the left-hand side are separated far enough to minimize the Coulomb interaction between different qubits. After two single-qubit operations (being performed in two separated pairs of quantum rings), rails leaving the AB quantum gates enter path selectors, which could either direct electrons to a position close enough to "turn on" the Coulomb interaction between them (for instance, the lightly shaded region in Fig. 1), or lead electrons away from the interaction region (then "turn off" the interaction). Path selectors can be realized by making the potential barrier on a certain path high enough or by a quantum circulator [8]. With a carefully designed length of the interaction region,

* Corresponding author. Tel.: +886 3 5712121x54174; fax: +886 35733722.
E-mail address: vam@faculty.nctu.edu.tw (O. Voskoboynikov).

0038-1098/$ - see front matter © 2007 Elsevier Ltd. All rights reserved.
doi:10.1016/j.ssc.2007.12.017

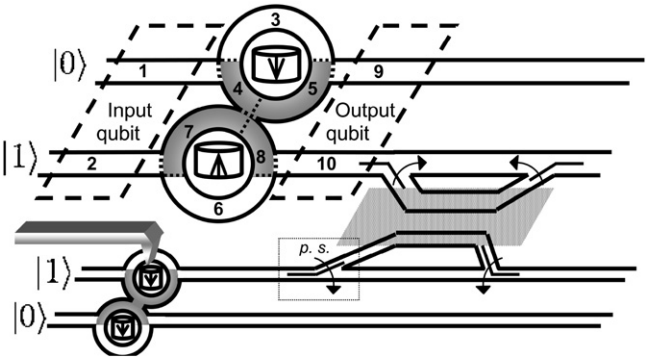

Fig. 1. Schematic diagram of the proposed architecture for quantum computation. Two pairs of parallel 1D quantum wires represent two qubits connected to two pairs of quantum rings, each of which stands for a single-qubit quantum gate. The upper pair demonstrates segments of the 1D quantum wave guides. The tablets in the rings are single-domain nano-sized magnets (the arrows indicate their magnetization), and the cantilever (for clarity reasons only one is shown) is used as a read-write head to monitor/control the magnetization. Path selectors (abbreviated as p.s.) are used to lead electrons to/away from the lightly shaded region (phase shifter), where the Coulomb interaction between electrons is strong enough to entangle two qubits. The numbers in the upper-left corner indicate the segments of the 1D quantum wires used in the calculation of a single-qubit gate.

the two qubits together will undergo a controlled phase shift transformation [3]. Since single- and two-qubit gates can be implemented, our architecture is scalable and can be expanded to perform arbitrary multi-qubit quantum computations [9]. From now on we focus on the construction of the single-qubit AB quantum gate in our discussion.

To determine the operations that a single qubit undergoes by passing the AB quantum gate, we evaluate the transmission matrix $\mathbf{T}$ between the input and output of the gate (see the upper-left corner of Fig. 1). Assuming singlemodedness in each segment j of the 1D quantum wave guides, we adopt the method proposed in [10], where the electron wave functions are represented by 1D plane waves. In the input and output leads (segments $j = 1, 2, 9, 10$ in Fig. 1) the electron wave vector is $k = \sqrt{2m^*E}/\hbar$, where E stands for the electron energy and m^* for the electron effective mass. The wave numbers of the plane wave solutions in the jth segment of the quantum wire (for $j = 3, 6$) are chosen to be $k_{i\pm} = k \pm \pi\phi_i/L$. Here the normalized flux ϕ is defined by $\phi_i = \Phi_i/\Phi_0$, where Φ_i is the magnetic flux through the upper ($i = 1$) or lower ($i = 2$) ring. $2L$ stands for the circumference of a quantum ring and "$\pm$" indicates whether the electron wave vector has the same direction as the magnetic vector potential or not. $\Phi_0 = \hbar/e$ is the universal flux quantum. In the segments $j = 4, 5, 7, 8$, their lengths are chosen to be $L/8$ and the electron wave number is given by $k_{i\pm} = k_g \pm \pi\phi_i/L$. The wave number k_g can differ from k and depends on changes in the chemical potential or the shape of the segment. Imposing the Griffith boundary conditions [10] at each intersection, one can determine the wave function of the whole structure and obtain the matrix elements T_{nm} of the transmission matrix, which relates the input and output electronic wave functions as

$$|0\rangle_{\text{out}} = T_{11}|0\rangle_{\text{in}} + T_{12}|1\rangle_{\text{in}}$$
$$|1\rangle_{\text{out}} = T_{21}|0\rangle_{\text{in}} + T_{22}|1\rangle_{\text{in}}.$$

Table 1
Error rate for the set of AB quantum gates

Gate	I	σ_z	σ_x	T	H
$\log_{10}\varepsilon$	−5.810	−5.810	−5.179	−5.810	−8.442
kL/π	0.839	0.839	0.839	0.839	1.219
ϕ_1	0.748	0.748	0.252	0.748	0.933
ϕ_2	−0.748	3.252	−0.252	0.252	−4.933

The last three rows define the dynamic working points for the gates, $\log_{10}(k_g/k) = 0.685$.

State $|0\rangle$ or $|1\rangle$ is the electronic wave propagating in the upper or lower rail correspondingly.

The probabilities of transmission $\mathbf{T}_0 = |T_{11}|^2$ from the input $\mathbf{0}$-rail to the upper and $\mathbf{T}_1 = |T_{12}|^2$ to the lower output rail for a particular k_g/k are shown in Fig. 2. The transmission probabilities are periodic functions of kL/π and ϕ_1 (ϕ_2 has the opposite sign to ϕ_1), so the plot region is chosen to cover exactly a period of ϕ_1. Our result shows that the quantum gate represented by the transmission matrix $\mathbf{T}$ is in general not unitary. With proper configurations of the AB quantum gates, however, not only is the transmission rate sufficiently high to perform a reasonably long quantum computation, but the resulting gate functionality can be changed dynamically. That T_0 and T_1 at $kL/\pi \approx 0.839$ attain their maximum for different ϕ_1 in Fig. 2 illustrates the dynamic change of the gate functionality by tuning the magnetic flux.

Using the AB quantum gates we can control directly the phase of the electronic wave function. Increasing the phase ϕ_1 by 1 changes the arguments of the matrix elements T_{11}, T_{12}, T_{21}, T_{22} by $-\frac{1}{4}\pi$, $-\frac{1}{8}\pi$, $-\frac{1}{8}\pi$, 2π, without affecting their moduli. Similarly, increasing the phase ϕ_2 by 1 changes these arguments by 2π, $\frac{1}{8}\pi$, $\frac{1}{8}\pi$, $\frac{1}{4}\pi$ respectively. Such a phase relationship is solely determined by the relative length of each segment in a ring, and can be designed to give a particular value of phase shift (e.g., a $-\frac{1}{4}\pi$ phase shift for T_{11} in our design). Therefore, with a proper choice of kL/π and k_gL/π, one can obtain a set of quantum gates of different functionality simply by varying ϕ_1 and ϕ_2 through the action of the cantilevers. It has to be noted that the AB quantum gates constructed in this way can only be symmetric. Asymmetric gates are achieved by connecting two or more gates in series.

In order to compare the error-prone (non-unitary) T-gates with ideal error-free (unitary) gates (U) we estimate the gate's error rate ε, which is defined as $\varepsilon = 1 - \mathrm{K}$, where $K = |\mathrm{Tr}(TU^\dagger)|/\mathrm{Tr}(UU^\dagger)$ is the gate fidelity [11]. We list a set of most common quantum gates and the corresponding working points in Table 1 for $\log_{10}(k_g/k) = 0.685$.

Fig. 3 shows the rich behavior of the minimal error rate ε (when ϕ_1 and kL/π are varied over the plot region in Fig. 2) as a function on k_g/k for σ_x and H, among other gates, for example. Clearly, the proposed AB quantum gates theoretically could demonstrate error rate $\varepsilon \to 0$ for a few k_g/k, when the electron ballistic transport and readout process are assumed to be ideal. Also, we take in the figure $\varepsilon_{th} = 10^{-4}$ as a rough estimate of the threshold for quantum computation, below which an arbitrarily large computation can be performed efficiently [9].

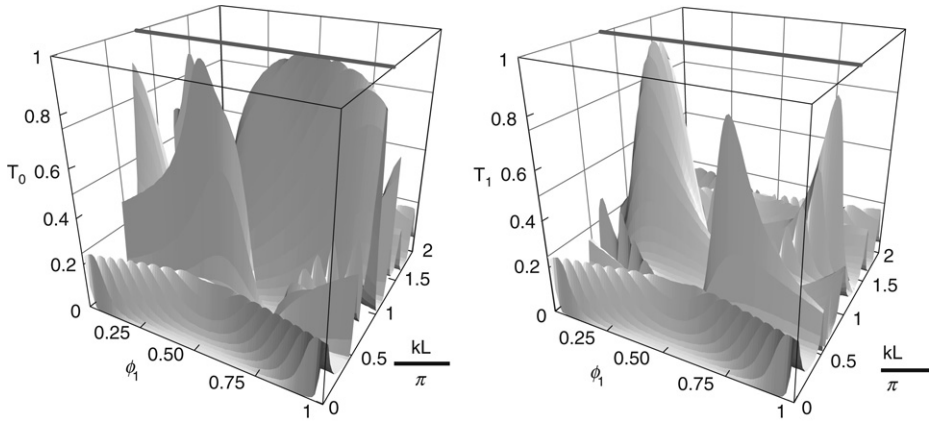

Fig. 2. Transmission probabilities from the **0**-rail of the input to the **0**-rail (left panel) and **1**-rail (right panel) of the output. $\phi_1 \cdot \phi_2 \leq 0$, $|\phi_1| = |\phi_2|$, $\log_{10}(k_g/k) = 0.685$. The gray line in the top plane is drawn for $kL/\pi = 0.839$.

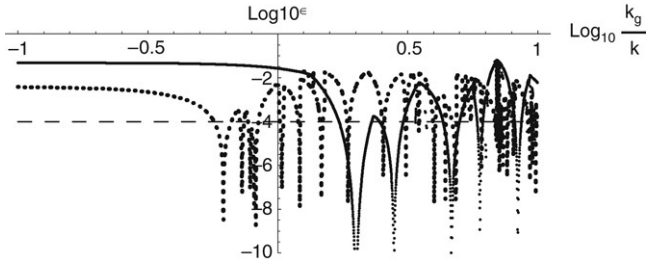

Fig. 3. Minimum error rate for the H and σ_x gates (dotted and solid line resp.). The horizontal dashed line stands for $\varepsilon_{th} = 10^{-4}$.

Moreover, due to the periodical behavior of the AB quantum gates described above, we conclude that the optimal operating points $(kL/\pi, k_gL/\pi, \phi_1, \phi_2)$ for a particular functionality can always be found by tuning and a very high fidelity can be achieved. In general, since the coupling between the two rings is controllable by k_g/k, any gate of the kind

$$\begin{pmatrix} \alpha & i\beta \\ i\beta & \alpha \end{pmatrix},$$

$\alpha, \beta \in R$ and $\alpha^2 + \beta^2 = 1$, can be represented by the AB quantum gates with high fidelity. With a general kind of gate (general gate), an *arbitrary* single-qubit quantum gate can be obtained by combining an AB quantum gate with additional single-qubit phase shifters. The possibility to choose and tune the gate dynamically makes our architecture particularly promising.

The proposed architecture can be implemented using two-dimensional electron gas structures and applying the split-gate techniques to define the pattern of 1D quantum wires. Within the dual rail representation for ballistic electron flying qubits, initialization and measurement of the qubit states can be done as was proposed in [3]. Nano-sized magnets can be electroplated on the sample [5]. Lithographic techniques enable us to make well-defined shapes and locations. The dynamic control of the AB quantum gates is realized by flipping the magnetization of the nano-magnets with read–write heads [12,13], possibly similar to MFM (magnetic force microscopy), which are shown in Fig. 1 as cantilevers. As a result we can manipulate the phase of the electronic wave functions. Further, different magnitudes of ϕ_1 and ϕ_2 are obtained by varying the size of the magnets and the rings, or by enclosing many magnets in a single ring. In addition, the application of the split-gate techniques to a two-dimensional electron gas makes the values of kL/π and k_gL/π tunable. Variation of the voltage applied to the gate changes the lateral confinement of the electrons in the quantum wires and modifies k and k_g. So, we can tune all four variables separately to choose the working point $k(L/\pi, k_gL/\pi, \phi_1, \phi_2)$ and to achieve the highest fidelity.

To be more concrete, the device size (i.e., the ring diameter) and the width of the quantum wires can be assumed to be 400 nm and 20 nm, respectively. Then about 20 nano-magnets with diameters 60 nm and spaced by 80 nm can be enclosed in a ring to provide up to several normalized magnetic fluxes (parameters are chosen as in [14]). Within the typically reported phase coherence length of 20 μm in the GaAs heterostructure [15], about 50 devices can be incorporated to perform a reasonably complex operation.

The approach proposed in [3] uses ballistic electrons. The functionality of the gates in that design is defined at the stage of fabricating the computer. This architecture will seriously suffer from any fabrication defect because defects cannot be compensated afterwards. In contrast, the dynamic controllability in our proposition implies that the functionality of each gate can be redefined after fabrication and even during operation. For instance one can dynamically reassign an H-gate into a T-gate during the calculation process. Since it is possible to make a hybridization of quantum computers and classical computers in solid state circuits, a classical computer is used to operate the read–write head. Without this dynamic re-programmability the architecture can only serve as special purpose quantum circuits but not as quantum computers for general purposes. We emphasize that the above advantages are entirely due to the universality of the AB quantum gates — multi-functionality is achieved by changing through k and k_g and the enclosed magnetic fluxes. The utilization of a magnetic field, rather than an electric field like in [3], has other benefits: low power, insensitivity to noise, and less stray field. We should note that non-uniformity in magnetic properties of the nano-magnets also can lead to certain decoherence during the gate's operation and re-assignation. Although a few

techniques recently have been developed for the fabrication of very uniform micro- and nano-scale arrays of low temperature permanent magnets [16,17], certainly the dynamic performance of such structures still needs to be improved.

In conclusion, we have proposed and analyzed an architecture for quantum computation with ballistic electrons: coupled ballistic Aharonov–Bohm quantum gates. On the one hand, such quantum gates can be tuned, controlled and reprogrammed dynamically. On the other hand, in properly selected operation regimes, the error rate of the gates approaches zero.

We would like to point out that our architecture can be used as a starting point for the implementation of dynamically reprogrammable quantum computers based on electrons as qubits and coupled quantum rings as quantum gates. On the other hand, the main idea to use an external magnetic flux as a dynamic factor to reprogram quantum computers during the calculation process is more general and potentially very rich. The rapid progress in the fabrication of quantum magnetic disks and the already elaborated high quality two-dimensional electron systems make us claim that quantum computation with ballistic Aharonov–Bohm quantum gates is not only promising but also feasible in the near future.

Acknowledgments

This work is supported by the National Science Council of Taiwan under contract NSC-95-2112-M-009-015. We wish to thank Dr. C. M. J Wijers for a critical reading of the manuscript.

References

[1] A. Bertoni, P. Bordone, R. Brunetti, C. Jacoboni, S. Reggiani, Phys. Rev. Lett. 84 (2000) 5912.
[2] J. Harris, R. Akis, D.K. Ferry, Appl. Phys. Lett. 79 (2001) 2214.
[3] R. Ionicioiu, G. Amaratunga, F. Udrea, Internat. J. Modern Phys. B 15 (2001) 125.
[4] Y. Aharonov, D. Bohm, Phys. Rev. 115 (1959) 485.
[5] S.Y. Chou, M.S. Wei, P.R. Krauss, P.B. Fischer, J. Appl. Phys. 76 (1994) 6673.
[6] I. Chuang, Y. Yamamoto, Phys. Rev. A 52 (1995) 3489.
[7] A. Bertoni, P. Bordone, R. Brunetti, C. Jacoboni, J. Modern Opt. 49 (2002) 1219.
[8] C.H. Wu, Diwakar Ramamurthy, Phys. Rev. B 65 (2002) 075313.
[9] M.A. Nielsen, I.L. Chuang, Quantum Computation and Quantum Information, Cambridge University Press, Cambridge, 2000.
[10] J. Xia, Phys. Rev. B 45 (1992) 3593.
[11] D. McHugh, J. Twamly, Phys. Rev. A 71 (2005) 012327.
[12] C.A. Ross, Annu. Rev. Mater. Res. 31 (2001) 203.
[13] C.A. Ross, H.I. Smith, T. Savas, M. Schattenburg, M. Farhoud, M. Hwang, M. Walsh, M.C. Abraham, R.J. Ram, Vac. Sci. Technol. B 17 (1999) 3168.
[14] R.P. Cowburn, A.O. Adeyeye, M.E. Welland, New J. Phys. 1 (1999) 161.
[15] G. Cernicchiaro, T. Martin, K. Hasselbach, D. Mailly, A. Benoit, Phys. Rev. Lett. 79 (1997) 273.
[16] W. Gillijns, M.V. Miloševic, A.V. Silhanek, V.V. Moschalkov, F.M. Peeters, Phys. Rev. B 76 (2007) 184516.
[17] M. Zheng, M. Yu, Y. Liu, R. Skomski, S.H. Liou, D.J. Sellmyer, V.N. Petryakov, Yu.K. Verevkin, N.I. Polushkin, N.N. Salashchenko, Appl. Phys. Lett. 79 (2001) 2606.